Complex Dynamics of Pyridinium Cation in Ferroelectric Bis(thiourea)pyridinium Iodide Studied by Quasi-Elastic Neutron Scattering

ARTICLE *in* THE JOURNAL OF PHYSICAL CHEMISTRY C · JULY 2011

Impact Factor: 4.77 · DOI: 10.1021/jp201940e

4 AUTHORS, INCLUDING:

Aleksandra Pajzderska
Adam Mickiewicz University
47 PUBLICATIONS **146** CITATIONS

SEE PROFILE

Jan Peter Embs
Paul Scherrer Institut
71 PUBLICATIONS **641** CITATIONS

SEE PROFILE

THE JOURNAL OF PHYSICAL CHEMISTRY C

ARTICLE

pubs.acs.org/JPCC

Complex Dynamics of Pyridinium Cation in Ferroelectric Bis(thiourea)pyridinium Iodide Studied by Quasi-Elastic Neutron Scattering

A. Pajzderska,*[,†] M. A. Gonzalez,[‡] J. P. Embs,[§] and J. Wąsicki[†]

[†]Faculty of Physics, A. Mickiewicz University, Poznań, Poland

[‡]Institute Laue Langevin, B.P. 156x, 38042 Grenoble Cedex 9, France

[§]Laboratory for Neutron Scattering, Paul Scherrer Institute, 5232 Villigen PSI, Switzerland

ABSTRACT: We have studied the dynamics of a bis(thiourea)pyridinium iodide inclusion compound by means of quasi-elastic neutron scattering (QENS). Our results reveal the complex dynamics of pyridinium cations confined in thiourea channels. Two types of pyridinium cation motions (in-plane and out-of-plane) were characterized in a wide temperature range using spectrometers with different energy resolutions. The QENS data allow description of the geometry of both motions and show that their corresponding correlation times differ more than 2 orders of magnitude at room temperature. The influence of the host thiourea matrix on pyridinium cation dynamics is discussed.

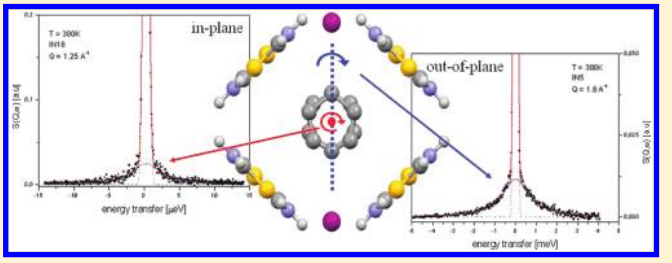

1. INTRODUCTION

Host−guest systems may form various types of inclusion compounds with different structures resulting in an effective confinement of the guest molecules. A variety of host molecules are able to form layer-type (two-dimensionally open), channel-type (one-dimensionally open), or cage-type (totally enclosed) inclusion compounds[1−3] In particular, channel-type solid organic inclusion compounds can be formed by urea, thiourea, perhydrotriphenylene, tri-*o*-thymotide, tetraphenylene, cyclodextrins, and others. It is worth noting that the empty urea and/or thiourea tunnel structure is unstable and the guest molecules are necessary to the stability of the host structure, which collapses if the guest molecules are removed.[1−4]

The urea and/or thiourea molecules form an extensive hydrogen-bonded honeycomb channel structure containing densely packed guest molecules[4,5] such as *n*-alkane chains, carboxylic acid (urea host), alicyclic and branched aliphatic hydrocarbons, adamantane, chloroform, carbon tetrachloride, or substituted benzene rings[6−12] (thiourea host). Another group of inclusion compounds is made by thiourea with pyridinium salts. In such compounds, the host lattice is built of ribbons of hydrogen-bonded thiourea molecules and iodide anions making channels of approximately square cross section and of a diameter close to 1 nm, in which the guest lattice pyridinium cations are located (Figure 1). Hitherto only four such systems have been found with the chloride, bromide, iodide, and nitrate anions.[13−16]

One-dimensional inclusion compounds formed by urea or thiourea present very interesting fundamental and physicochemical properties. Their incommensurate properties,[6,17−19] the character of their phase transitions,[12,20,21] and the dynamics of guest molecules[19,22−24] were studied by X-ray and neutron diffraction, nuclear magnetic resonance, and inelastic neutron scattering methods. MD simulations have investigated the dynamics of guest molecules as well.[18,25−30]

We have focused our attention on the inclusion compounds of thiourea with pyridinium salts. Recently, we have characterized the guest-lattice reorientation in bis-thiourea pyridinium nitrate and chloride. The pyridinium cation undergoes two types of reorientations: (i) out-of-plane motions and (ii) in-plane motions about an axis perpendicular to the plane of the cation.[15,32−34] The correlation time of the former motion has been estimated to be of the order of some picoseconds, while the correlation time of the in-plane motion is on the order of nanoseconds at room temperature.

The out-of-plane motion has been characterized as a function of temperature by ^{1}H NMR, dielectric, and QENS methods in bis(thiourea)pyridinium chloride.[34] The reorientation of the pyridinium cation takes place about the axis passing through two opposite atoms of the ring. The in-plane motion was studied by ^{1}H, ^{2}H NMR, and QENS in the bis(thiourea)pyridinium nitrate compound.[34,35] The in-plane motion of the cation could not be described by a simple model involving rotations about equivalent barriers as only a more complex model taking into account the existence of three preferred positions due to the formation of H-bonds between the pyridinium guest and the host matrix could

Received: February 28, 2011
Revised: June 27, 2011
Published: July 03, 2011

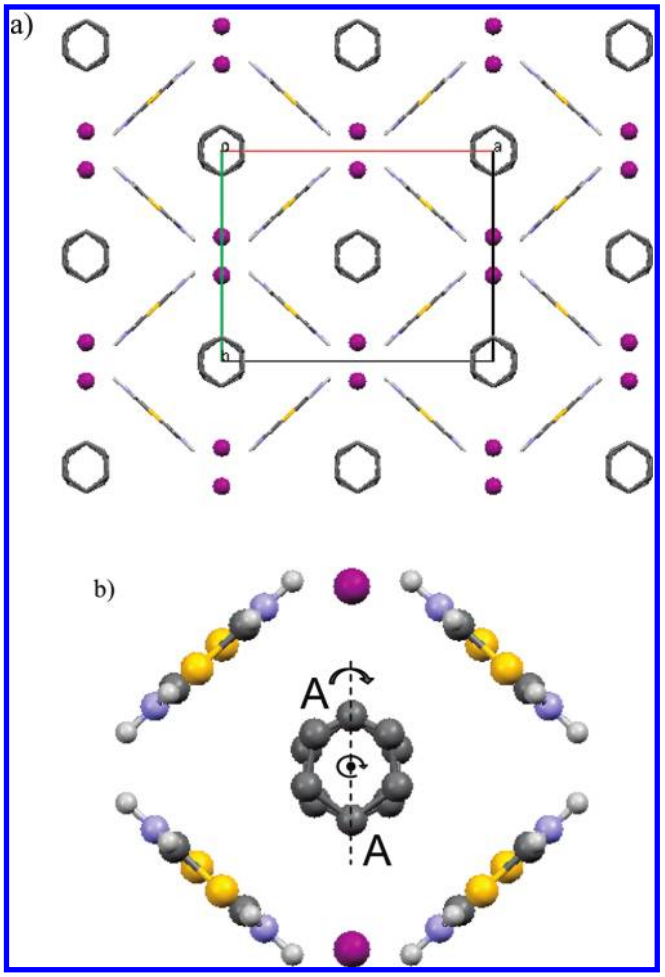

Figure 1. (a) The structure of bis(thiourea)pyridinium iodide inclusion compound at 300 K, viewed along the *c* axis. For clarity hydrogen atoms in pyrdinium have been omitted.[31] (b) The thiourea channel and a disordered pyridinum cation. Two axes of reorientation are depicted: the axis passing through two atoms A and the axis perpendicular to the cation's plane.

reproduce the experimental EISF (the elastic incoherent structure factor).[32]

These results show that the guest−host interaction strongly influences the geometry of the motions occurring in these inclusion compounds. Therefore it is interesting to determine how the dynamics of the pyridinium cation is affected by the replacement of the host anion, so we have explored the compound formed with iodide, which has a spherical shape in contrast to the flat shape of the nitrate anion.

Thus, the subject of our study is bis(thiourea) with pyridinium iodide $[(SC(NH_2)_2)_2(C_5NH_6)]^+I^-$ (hereafter T_2(PyH)I). DSC measurements performed in the range 100−400 K showed the occurrence of two phase transitions at 141 and 161 K and dielectric measurements revealed ferroelectric properties on this compound.[31] On the basis of X-ray data, the following sequence of space groups was obtained: $Cmcm \rightarrow C2cm \rightarrow P2_1cn$.[31] As mentioned above, this compound is built of two sublattices: that of the guest (pyridinium cations) and that of the host (thiourea molecules and iodine anions). The thiourea molecules linked by the N−H···S hydrogen bonds are arranged head-to-tail, forming ribbons along the *z* axis. Each ribbon is made of two halves that are parallel in the high-temperature phase or make an angle of 12° in the intermediate phase or 17° in the low-temperature phase. Four such ribbons form a channel of approximately square cross section and a size along the diagonal of about 1 nm, containing the pyridinium cations. The angle made by the pyridinium cation plane and the (001) crystal plane (the cross section of the channel) in the high-temperature and intermediate phases is 90°, while in the low-temperature phase is 82.4°.[31]

The aim of our study is to investigate in detail the dynamics and geometry of reorientation of the pyridinium cation in the T_2(PyH)I compound. From the behavior of the chloride and nitrate counterparts, it was expected that the pyridine cation would perform two types of motion as well, these are the in-plane and out-of-plane reorientations. Therefore quasi-elastic neutron scattering measurements were performed on different spectrometers having considerably different resolutions, making it possible to draw conclusions on the complex motion of the pyridinium cation in T_2(PyH)I.

The data obtained for the thiourea pyridinium iodide inclusion compound are also compared with the published results for pyridium iodide (hereafter (PyH)I),[35] in order to obtain a clear measure of the influence of the environment on the cation dynamics in confined geometry.

2. EXPERIMENTAL SECTION

The quasi-elastic neutron scattering (QENS) measurements of T_2(PyH)I were performed on the backscattering spectrometers IN10 and IN16 and on the time-of-flight spectrometer IN5 at the Institut Laue Langevin, Grenoble.

For the backscattering spectrometers the incident wavelength was 6.27 Å allowing exploration of the Q-range between 0.2 and 1.96 $Å^{-1}$ and the energy range ±10 μeV with an energy resolution of 0.9 μeV (fwhm). Measurements on IN16 were performed at 155 K (intermediate phase) and 300 K (high temperature phase), while on IN10 we acquired data at eight temperatures in the range 10−350 K. It must be noted that even if both spectrometers have similar characteristics in term of *Q*-range and resolution, IN16 has a larger number of detectors than IN10 (22 vs 7) and a better signal-to-noise ratio, so only the IN16 data were employed to extract the experimental EISF and select the model of motion as explained in the text. In the measurements performed on the time-of-flight spectrometer IN5, the incident wavelength was 5 Å and the energy resolution was 150 μeV (fwhm). The *Q* range covered was 0.6−2.2 $Å^{-1}$ and the energy range used in the analysis was from −5 to 4 meV.

A polycrystalline sample was prepared as described in ref 13 and placed in an aluminum flat slab holder of size 4 × 3 cm^2 and thickness 0.35 mm. The sample mass was about 0.67 g, which was selected to ensure a transmission coefficient between 0.85 and 0.9 in order to minimize multiple scattering. The angle between the sample surface and the beam of incident neutrons was 135° for all cases. Raw data were treated with the program LAMP.[36] The background was subtracted using a measurement of the empty sample container and taking into account sample absorption. Then, using a vanadium spectrum as an incoherent elastic scattering standard, the intensities were normalized for detector efficiency and transformed to energy scale. As the IN16 spectrometer permits simultaneous measurement of the quasi-elastic spectrum and the diffraction pattern, the QENS spectra

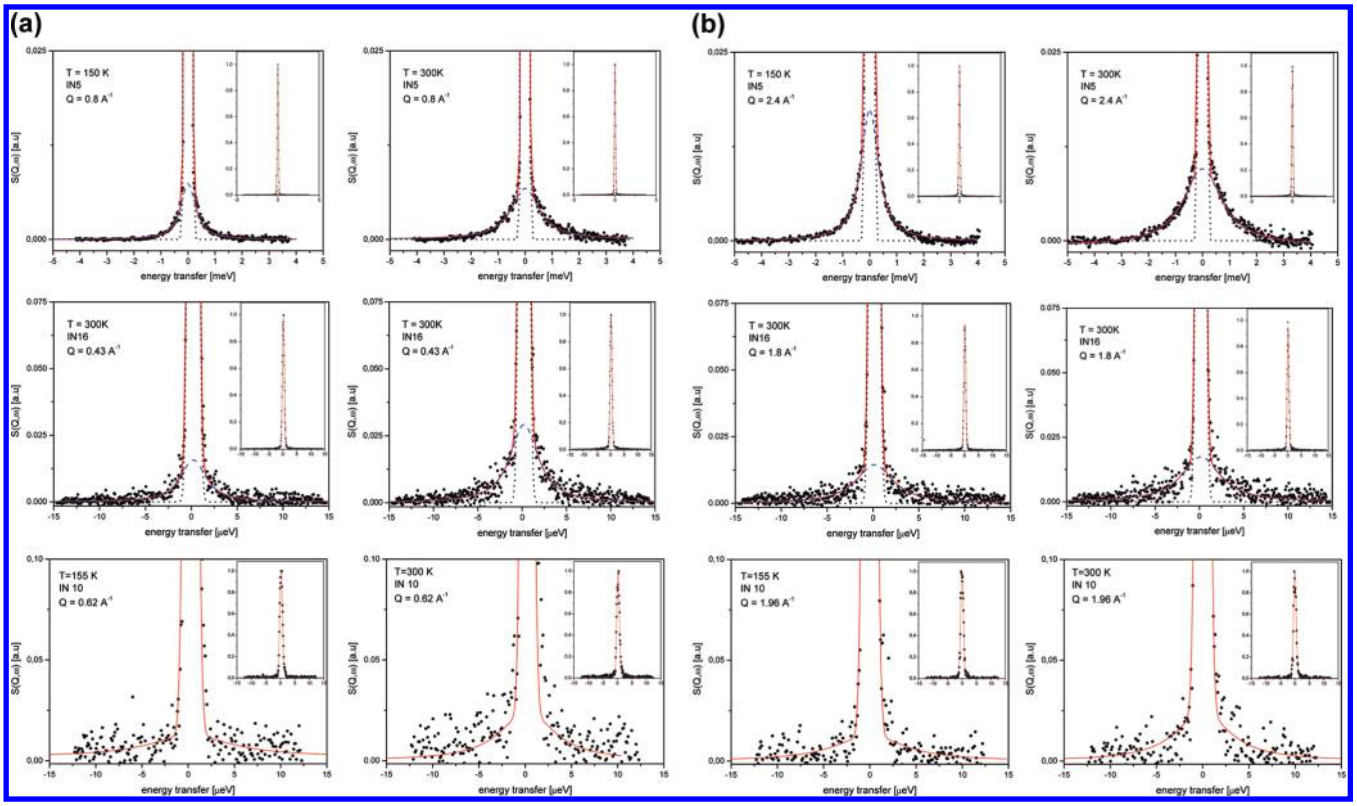

Figure 2. QENS spectra for T_2(PyH)I measured on IN5 (top), IN16 (middle), and IN10 (bottom) spectrometers at 155 and 300 K (a) at lower Q values (b) at higher Q values. (b) For IN5 and IN16 spectra the solid line shows the fitted spectra, the dotted line corresponds to the resolution function, and the dashed line is the quasi-elastic contribution. For the IN10 spectra the solid line shows the fitted spectra using a model of jumps between two nonequivalent sites (eq 8). The entire fitted spectra are shown in the inset.

corresponding to Q contaminated by the elastic coherent scattering originated from Bragg reflections of the sample were excluded from data evaluation.

3. THEORY

Quasi-elastic neutron scattering experiments measure the dynamic structure factor, $S(\mathbf{Q}, \omega)$, which is the Fourier transform of the intermediate scattering function $I(\mathbf{Q}, t)$.[37] The dynamic structure factor contains a sum of coherent and incoherent contributions, but in samples containing hydrogen the large incoherent scattering cross section of this element dominates the total scattering and one measures basically the Fourier transform of the self-intermediate scattering function, $I_s(\mathbf{Q},t) = \langle e^{-i\mathbf{Q}\mathbf{r}(0)} e^{i\mathbf{Q}\mathbf{r}(t)} \rangle$. The long time limit $I_s(\mathbf{Q},t\rightarrow\infty)$ is called the elastic incoherent structure factor (EISF) and represents the probability of finding the scatterer in a volume $\propto 1/Q$ around $\mathbf{r}_0$ at infinite time. Thus the EISF is related to the region of the space accessible to the scatterers and yields direct information about the geometry of their motions.[37] Splitting the self-intermediate scattering function into time-independent and time-dependent parts, we have $I_{inc}(Q,t) = I_{inc}(Q,\infty) + I_{inc}'(Q,t)$ and its Fourier transform gives $S_{inc}(Q,\omega) = I_{inc}(Q,\infty)\,\delta(\omega) + S^{q}_{inc}(Q,\omega)$, so experimentally the EISF is simply obtained as[38]

$$\mathrm{EISF}(Q) = \frac{S^{el}(Q)}{S^{el}(Q) + S^{q}(Q)} \qquad (1)$$

In all cases the spectra were fitted with the following expression (convoluted with the resolution function $R(Q,\omega)$)

$$S(Q,\omega) = A_0(Q)\delta(\omega) + (1 - A_0(Q))L(\omega) + B(Q,\omega) \qquad (2)$$

where A_0 is the EISF, $L(\omega)$ is a Lorentzian function of width τ^{-1} (proportional to the correlation time), and $B(Q,\omega)$ describes the background.

4. RESULTS AND DISCUSSION

4.1. Data Analysis. The quasi-elastic spectra obtained were fitted by expression 2. The resolution function was well approximated by a Gaussian function, and an additional background was employed to fit the spectra measured on IN5. Figure 2 shows representative examples of the data obtained at two different temperatures with the three spectrometers used in this work and the corresponding fits. In the high and intermediate temperature phases a quasi-elastic broadening is clearly visible in all the cases, whereas for the low-temperature phase only the spectra taken on IN10 and IN16 show a small QENS component, which is not visible at temperatures below 135 K. The width of the Lorentzian function $\Gamma(Q)$ at a given temperature does not show any Q dependence within the limit of the error. This behavior suggests a model of reorientation by jumps between two or three positions, for which the quasi-elastic broadening is Q-independent and proportional to the rate of jumps $1/\tau_c$. The estimated correlation times for the in-plane and out-of-plane motions in the

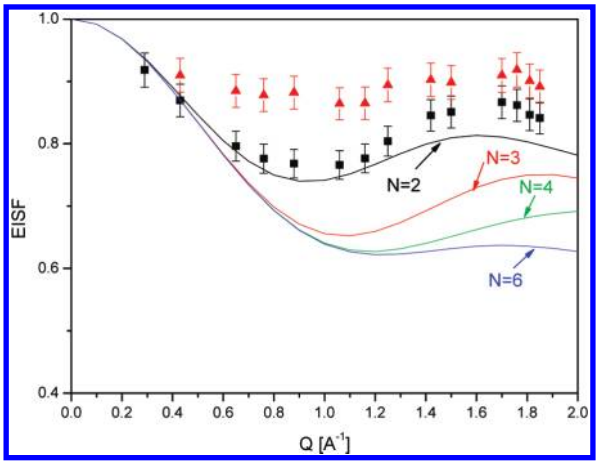

Figure 3. Experimental elastic incoherent structure factor (EISF) obtained in a model independent way at (black solid square) 300 K and (red solid triangle) 155 K from IN16 measurements. The solid lines correspond to the different models of jumps between N equivalent sites, calculated from eq 4.

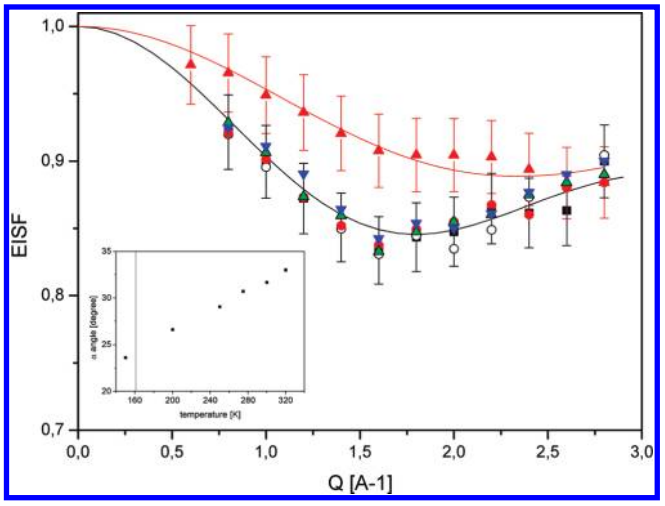

Figure 4. Experimental elastic incoherent structure factor (EISF) obtained in a model independent way at (open circle) 320 K, (black solid square) 300 K, (red solid circle) 275 K, (green solid triangle) 250 K, (blue solid triangle down) 200 K, and (red solid triangle) 150 K from IN5 measuremets. The solid lines show the best fit of the model corresponding to the out-of-plane motion (eq 9) at 300 and 150 K. The inset shows the temperature dependence of the angle α.

high-temperature phase at 300 K are of the order of nano- and picoseconds, respectively. It should be emphasized that the correlation times of both motions differ by more than 2 orders of magnitude. As the intensity $A_0(Q)$ in eq 2 is directly equal to the elastic incoherent structure factor (EISF), this fit permits determination of the EISF in a model independent way. The EISF derived from the IN16 data, which corresponds to the slower motion (in-plane) is shown in Figure 3, while Figure 4 shows the EISF corresponding to the out-of-plane motion.

It should be noted that the backscattering data were also fitted taking into consideration a second Lorentzian function corresponding to the fast motion observed on the time-of-flight spectrometer. The inclusion of this component in the fit did not change the value of the EISF obtained, which follows from the fact that the time scale of this fast motion, and hence the width of the Lorentz function, differs by 2 orders of magnitude from that of the process observed on IN10 or IN16. For the same reason, the use of a narrow Lorentzian having a width ~0.003 meV at 155 K and ~0.008 meV at 350 K derived from the backscattering data does not introduce any change in the parameters obtained from the fit of the IN5 data.

The EISFs obtained at 300 K (high-temperature phase) and at 155 K (intermediate phase) at IN16 present a minimum at Q = 0.9 Å^{-1} and a maximum at Q = 1.6 Å^{-1}. The main difference between the two phases is the depth of the oscillations observed, which are much more pronounced for the high temperature phase. The EISF obtained from the measurements on IN5 in the high-temperature phase has a minimum at 320 K for Q = 1.7 Å^{-1}. Decreasing the temperature causes a shift of the minimum toward higher Q and at 150 K (the intermediate phase) the minimum occurs at Q = 2.6 Å^{-1}.

The EISF obtained contains contributions from all atoms in the sample and can be written as the sum of the contributions from the three types of molecules and/or ions in the sample: thiourea, pyridinium cations, and iodide anions. However, the contribution from iodide anions (which represents less than 0.5% of the total scattering signal) can be neglected and as 90% of the scattering is due to protons so we have

$$\begin{aligned} \mathrm{EISF} &= \left(\frac{8}{14}\right)A_0^{thio} + \left(\frac{6}{14}\right)A_0^{Py} \\ &= \left(\frac{8}{14}\right) + \left(\frac{6}{14}\right)A_0^{Py} \end{aligned} \tag{3}$$

where $A_0^{\mathrm{thio}} = 1$ because the thiourea molecules do not diffuse in the time scale of the experiment and therefore scatter purely elastically, A_0^{Py} is the EISF corresponding to the pyridinium cation, and 6, 8, and 14 are the numbers of hydrogen atoms in the pyridinium cation, in the thiourea molecule, and in the total scattering unit. Then by comparing the experimentally extracted A_0^{Py} with the expressions corresponding to different models of motion it is possible to find the model that provides a better description of the experimental data.

Taking into regard the results of our earlier studies for bis(thiourea)pyridinium nitrate and chloride, two types of motions were considered: (a) in-plane motion and (b) out-of-plane motion.

4.2. Analysis of In-Plane Motion—Jumps around the Axis Perpendicular to the Pyridinium Cation. *4.2.1. Jumps among N Equivalent Sites on a Circle—Reorientation through Equivalent Barriers.* At first the pyridinium cation was assumed to perform reorientations about the axis perpendicular to its plane between N equivalent positions. For such a model[37] taking into account eq 3, the EISF for a polycrystalline sample takes the form

$$\mathrm{EISF} = \left(\frac{8}{14}\right) + \left(\frac{6}{14}\right)\left[\frac{1}{N}\sum_{n=1}^{N} j_0\left(2Qr\sin\frac{n\pi}{N}\right)\right] \tag{4}$$

where j_0 is the zeroth-order spherical Bessel function, r is the radius of the circle of rotation, and N is the number of equivalent positions. For pyridinium r is equal to the distance from the center of gravity of the cation to the hydrogen atom and was fixed as r = 2.4 Å. Then jumps through two, three, four, and six equivalent positions were considered.

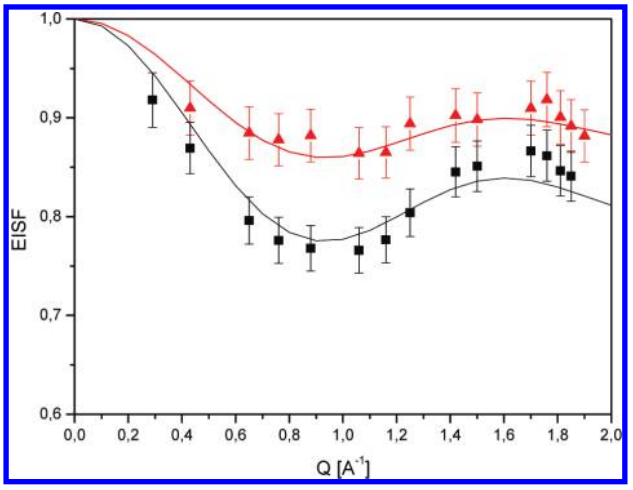

Figure 5. Experimental elastic incoherent structure factor (EISF) obtained in a model independent way at (black solid square) 300 K and (red solid circle) 155 K from IN16 measurements. The solid lines show the best fit of the in-plane motion by the model of jumps between two nonequivalent sites (eq 5) with $p_1 = 0.71$ at 300 K and 0.84 at 155 K.

Figure 3 presents the experimental EISF for the high (300 K) and intermediate (155 K) temperature phases and the theoretical dependence calculated according to eq 4 for $N = 2, 3, 4, 6$. Only the model with $N = 2$ produces a theoretical EISF presenting a minimum and a maximum at the right Q values, but the model is not able to account quantitatively for the dependence observed experimentally. Furthermore the differences between the experimental EISFs obtained at 155 and 300 K indicate either that the geometry of the motion is not the same in the high- and intermediate-temperature phases or that some temperature-dependent parameter needs to be introduced in the model to account for those differences.

4.2.2. Jumps among N Nonequivalent Sites on a Circle—Reorientation through Nonequivalent Barriers. Therefore we decided to analyze the possibility of having jumps between inequivalent positions distributed over a circle of radius r. As before the axis of rotation is perpendicular to the plane of the cation and the radius of the circle is 2.4 Å (the distance between the center of the ring and the hydrogen atom). But now the cation can take certain positions with different probabilities p_i ($i = 1, ..., N$ and $\Sigma_{i=1}^{N} p_i = 1$). For this model, the EISF (averaged for a powdered sample and taking into account eq 3) can be written as[39]

$$\mathrm{EISF} = \left(\frac{8}{14}\right) + \left(\frac{6}{14}\right)\left[\sum_{i=1}^{N}\sum_{j=1}^{N} p_i p_j j_0\left(2Qr \sin\left|\frac{n}{N}(i-j)\right|\right)\right] \quad (5)$$

The use of different probabilities modifies the height of the theoretical EISF but not the position of the minima and maxima. Therefore we can disregard the models with $N > 2$ and focus on the model corresponding to 180° jumps between two nonequivalent positions. And as shown in Figure 5, this model can describe in a satisfactory way the experimental EISF obtained at both temperatures. In the high-temperature phase the probabilities obtained are $p_1 = 0.71$ and $p_2 = 0.29$, while in the intermediate phase we have $p_1 = 0.84$ and $p_2 = 0.16$. Passing from the intermediate to the high-temperature phase, the probabilities change and the inequivalence of population decreases. The small

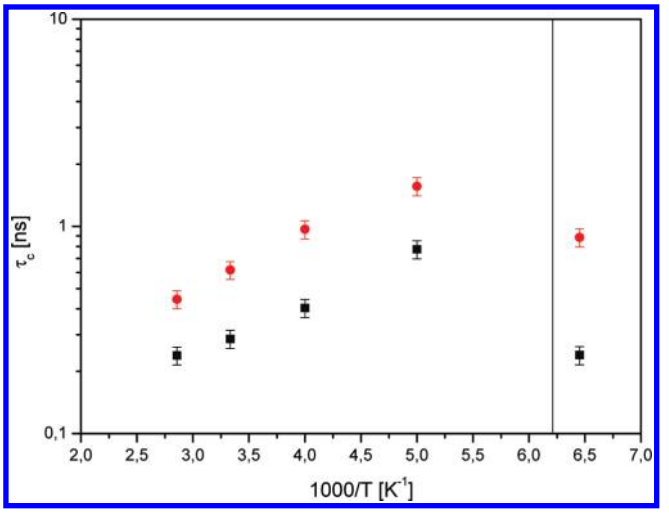

Figure 6. The correlation times τ_1 (red solid circle) τ_2 (black solid square) obtained from fitting the model (eq 8) to the IN10 spectra.

disagreement for Q around 1.7 Å^{-1} can be explained by the presence of Bragg peaks in this range.

It is also interesting to explore the temperature variation of the parameters describing the model of motion so the measurements obtained on the IN10 spectrometer at 10, 100, 135, 155, 200, 250, 300, and 350 K were analyzed using the theoretical expression for $S(Q,\omega)$ corresponding to a model of jumps between two nonequivalent positions. The quasi-elastic broadening is well seen in the high and intermediate phases, whereas in the LT phase at 135 K the broadening is weak and at lower temperatures is not detected. The model of jumps between two inequivalent jumps has been presented by refs 37 and 40 and has been used by many authors, e.g., ref 41. In this model two different residence times $\tau_1 \neq \tau_2$ can be introduced, and their reciprocals $1/\tau_1$, $1/\tau_2$ are equal to the probabilities of jumping from one site to another. The probabilities of populations of the two positions are p_1 and p_2, respectively, the sum of these probabilities is $p_1 + p_2 = 1$, and finally $p_1/\tau_1 = p_2/\tau_2$ holds. Denoting the depth of the first minimum by E_A and the other one by E_B, the difference between them is the asymmetry parameter

$$\Delta = E_A - E_B = RT \ln \frac{p_1}{p_2} \quad (6)$$

where R is the gas constant and T the temperature. The corresponding dynamic structure factor is given by

$$S(Q,w) = A_0 + (1 - A_0)L(\Gamma) \quad (7)$$

Taking into account the rigid thiourea molecules (eq 3), $A_0(Q)$ is given by

$$A_0(Q) = \frac{8}{14} + \frac{6}{14}\left(\frac{1}{(p_1 + p_2)^2}[p_1 p_1 + p_2 p_2 + 2p_1 p_2 j_0(2Qr)]\right) \quad (8a)$$

and the width of the Lorentzian function is

$$\Gamma = \frac{1}{\tau_1 p_2} = \frac{1}{\tau_2 p_1} \quad (8b)$$

The spectra obtained on IN16 and IN10 spectrometers were fitted at all temperatures with eq 2, but using $A_0(Q)$ from eq 8. A

typical example of the fits obtained from the IN10 spectra is shown in Figure 2, providing evidence of the good agreement between the experimental data and the model assumed. At comparable temperatures, the parameters obtained from the fit of IN10 and IN16 spectra are in good agreement, as well. In the high temperature phase the probability of each population depends weakly on the temperature (p_1 = 0.65 at 350 K, p_1 = 0.68 at 300 K, p_1 = 0.71 at 250 K, p_1= 0.72 at 200 K) and changes at the phase transition p_1 = 0.79 (155 K) and p_1 = 0.85 (135 K). According to (8b), knowing the probabilities of populations and the width of the Lorentzian function at a given temperature, it is possible to establish the temperature dependence of the two correlation times (Figure 6). We can observe that the correlation time corresponding to the intermediate temperature phase is shorter than in the high temperature one. Even if surprising, this is consistent with the results obtained in a previous NMR study,[14] which showed a slowing down of the pyridinium cation reorientation at the transition from the intermediate to the high temperature phase. In the high temperature phase the activation energies obtained from the Arrhenius equation are E_A = 5.7 kJ/mol and E_B = 3.9 kJ/mol (i.e., Δ = 1.8 kJ/mol).

While this model fits nicely the experimental data, it raises the question of why such a geometry of motion and hence such a shape of the potential are preferred if the cation symmetry (pseudo-6-fold) should favor the jumps between six positions separated by 60°. It is supposed that an important reason for this is the effect of the host sublattice. To verify this supposition the crystallographic structure of the system was analyzed. The X-ray measurements did not permit determination of the nitrogen position in the cation, proving again the cation's dynamical disorder. In the high-temperature phase the cation's position has 2/m site symmetry. The carbon atoms, labeled in Figure 1 by the letter A are crystallographically equivalent and their distance to the iodide atom is 3.921 Å. These two carbon atoms have well-defined positions, and each of them appears as one single atom. On the other hand the remaining four atoms in the crystal structure give eight positions so each of them is split into a doublet. Therefore, it seems likely that because of the electrostatic cation−anion interactions the nitrogen atoms occupy one of the two positions labeled as A. As in the high-temperature phase the distance to the I anion is the same for both positions, and one would expect that both minima have the same populations. However, the Fourier transform of the X-ray diffraction pattern is the electron density of the crystal averaged over space and time, and if motions are slow on the X-ray time scale, they will make only a minimal contribution to the average electron density.[42,43] The pyridinium cation undergoes reorientations and is dynamically disordered. Temporarily, because of the cation motion, the cation−anion distance can be reduced and then one of the minima will be more populated. On the other hand in the intermediate phase the pyridinium cation is also dynamically disordered and has 2 site symmetry. This means that the same carbon atoms above-mentioned are not crystallographically equivalent. The distances between them to the iodide ions are 3.749 and 3.999 Å, justifying the different jump probabilities observed.

4.2.3. The Problem with the Resolution Effect. The model of jumps between two nonequivalent positions separated by 180° is in good agreement with the experimental data. But another possibility is that the probabilities of occupation of both sites are identical but not all the pyridinium cations contribute to the observed quasi-elastic broadening due to the limited instrumental resolution. Lechner[44] reported on the effect of the spectrometer resolution on the intermediate scattering function and EISF values. In this case we would have

$$\mathrm{EISF} = \left(\frac{8}{14}\right) + \left(\frac{6}{14}\right)\left[c + (1-c)\frac{1}{N}\sum_{n=1}^{N} j_0\left(2Qr\sin\frac{n\pi}{N}\right)\right] \quad (9)$$

where c represents the fraction of pyridinium cations that are not mobile on the time scale of the measurement. Mathematically this model is completely equivalent to the one represented by eq 5 for N = 2, so no distinction between them can be done solely on the basis of the quality of the fitting. In the high-temperature phase, we obtain c = 0.12, while in the intermediate phase we get c = 0.50. This implies that because of the limited resolution of the spectrometer, the intermediate scattering function does not decay completely to the expected equilibrium value, causing 12% and 50% of the pyridinium cations appear as immobile, even if they are all equivalent.

4.3. Analysis of Out-of-Plane Motion—Reorientation about the Axis Passing through Two Opposite Atoms of the Pyridinium Cation by ± α deg. This model assumes that the axis of rotation is in the cation's plane and passes through two opposite atoms of the pyridinium cation and that the cation can perform jumps between two positions separated by d (so their amplitude is α). Because of the dynamic disordering of the cations, in the intermediate and high-temperature phase the nitrogen atom positions are crystallographically indistinguishable. Upon this motion two hydrogen atoms are on the axis of rotation, and the EISF is given by the following formula[34,37]

$$\begin{aligned}\mathrm{EISF} &= \left(\frac{8}{14}\right) + \left(\frac{6}{14}\right)\left[\frac{2}{6} + \left\{\frac{4}{6}\left(\frac{1}{2} + \frac{1}{2}j_0(Qd)\right)\right\}\right] \\ &= \left(\frac{8}{14}\right) + \left(\frac{6}{14}\right)\left[\frac{2}{6} + \left\{\frac{4}{6}\left(\frac{1}{2} + \frac{1}{2}j_0(2Qr\sin(\alpha))\right)\right\}\right]\end{aligned} \quad (10)$$

where $j_0(x)$ is the spherical Bessel function of zeroth order, d is the distance between two positions, r is the radius of the pyridinium cation, and α is the amplitude of the out-of-plane motion.

Figure 4 presents the best fit to the experimental data obtained with eq 10, and the inset shows the angle α as a function of temperature. With increasing temperature the amplitude of motion increases linearly in the high-temperature phase passing from 27° at 200 K to 34° at 320 K. In the intermediate phase α = 23°, and the EISF can be fitted only assuming jumps between nonequivalent positions (p_1 = 0.78, p_2 = 0.22) or that not all the molecules are mobile in the time scale of the instrument (c = 0.37). The correlation time for this motion in the intermediate phase is $\tau_c^{out} \approx$ 3.1 ps (at 150 K). In the high-temperature phase the correlation time decreases with increasing temperature. From the analysis of IN5 data we obtain $\tau_c^{out} \approx$ 1.9 ps at 300 K and 2.8 ps at 200 K. Assuming an Arrhenius law, the activation energy E_a is estimated as 2.0 kJ/mol.

In this model we do not specify the exact opposite atoms through which the rotation axis passes. However, an analysis of the structural data suggests that the cation reorients about the axis passing by atoms labeled by A in Figure 1 leaving unaffected their positions and causing the splitting of the other four carbons.

4.4. The Comparison with Pyridinium Iodide. The QENS measurements permit characterizations of the complex dynamics of the pyridine cation in the inclusion compound of bis(thiourea)

with pyridinium iodide. The cation performs two types of motion: in-plane and out-of-plane reorientations and the frequencies of these two motions differ by 2 orders of magnitude at room temperature. It is interesting to compare the dynamics of the pyridinium cation confined in the thiourea matrix and in pure pyridinium iodide ((PyH)I). This compound presents a phase transition at 250 K[45] and the dynamics of the pyridinium cation has been studied above and below the phase transition by NMR[45,46] and QENS.[35] It should be underlined that there are no experimental reports on the out-of-plane motion of the pyridine cation in (PyH)I. In particular, it has not been detected by QENS or by ^{2}H NMR methods. For pure pyridinium nitrate the analysis of ^{2}H NMR line shape does not show any indication of such a motion either.[33] Therefore, it can be concluded that this out-of-plane motion is characteristic only of cations confined in thiourea channels.

QENS measurements on pyridinium iodide were done by Mukhopadhyay et al. using a time-of-flight spectrometer with two different resolutions: 17 and 6.5 μeV.[35] Those authors took data in the high-temperature phase (296, 270 K) and below the phase transition, at 240 K. They interpreted the motion in the high-temperature phase as the reorientation of the cation about the axis perpendicular to its plane through 6 equivalent positions, which is in agreement with NMR results,[45,46] but they did not interpret the cation dynamics below the phase transition. In this phase the value of the EISF increased considerably. In view of our above considerations (section 4.2), the reasonable conclusion is that the pyridinium cation either performs reorientations through nonequivalent barriers or the frequency of its motion has decreased so much that a large fraction of the molecules appears as immobile.

The correlation times for (PyH)I obtained at 296 and 270 K are 41.1 and 73.1 ps, respectively, so they are about 1 order of magnitude shorter then those obtained for T_2(PyH)I. This result indicates that the confinement of the pyridinium cations in the inclusion complex slows down their reorientation. The activation energy estimated for (PyH)I from the QENS measurements in the high-temperature phase is 14.7 kJ/mol, which is in good agreement with that determined from NMR measurements and much higher than that found in T_2(PyH)I.

The host sublattice has a significant influence on the geometry of the cation motion. In (PyH)I, in HT phase, the jumps take place through six equivalent positions, so the jumps are in agreement with the cation symmetry (pseudo-*C*6). In T_2(PyH)I and T_2(PyH)NO_3 the cation undergoes reorientations through two (at 180°) and three (at 120°) positions.

In T_2(PyH)NO_3 the three preferred positions were related to the formation of hydrogen bonds with the host matrix, that is with NO_3 anions and thiourea molecules. It should be emphasized that in this complex, even in the high-temperature phase, the walls built by the thiourea molecules are not planar, thus permitting the formation of hydrogen bonds. In T_2(PyH)I the thiourea walls are planar in the high-temperature phase and almost planar in the intermediate phase, so the distance between the pyridinium cations and thiourea molecules is larger and the formation of hydrogen bonds is suppressed. Analysis of the crystallographic structure of the complex indicates the close contact with iodide anions, thus favoring the 180° jumps. Thus, the experimental results suggest that in T_2(PyH)I the Coulomb interactions play an essential role on determining the geometry of the cation motion.

5. CONCLUSIONS

The above presented and discussed QENS results for T_2(PyH)I allow the following conclusions to be drawn.

1. The pyridinium cation performs two types of motion, slow in-plane and rapid out-of-plane, with correlation times differing by about 2 orders of magnitude.
2. In the intermediate and high-temperature phases, the in-plane reorientation of the pyridinium cation takes place between two minima of potential energies separated by 180°, about the axis perpendicular to the cation's plane. At 300 K the jumping times from each minimum are calculated to be 0.3 and 0.6 ns, and the activation energies are E_A = 5.7 kJ/mol and E_B = 3.9 kJ/mol.
3. The out-of-plane motion of the pyridinium cation takes place about the axis passing through two opposite atoms of the cation. The amplitude of this motion is 33°, the correlation time is estimated as 1.9 ps, and the activation energy is 2.0 kJ/mol.
4. Comparison of the pyridinium cation dynamics in thiourea channels and in the pure PyHI salt has shown that the confinement in thiourea channels affects significantly the geometry of the motion, slows down the in-plane reorientation of the cation and reduces the activation energy, and induces the appearance of an out-of-plane motion of the cation.

■ ACKNOWLEDGMENT

The authors thank Professor R. Lechner for his kind advice and very fruitful discussions. The work has been partially financed by the Ministry of Science and Higher Education of Poland, Grant No. 202 032937.

■ REFERENCES

(1) Atwood, J. L. Inclusion (Clathrate) Compounds. In *Encyclopedia of Physical Science and Technology*, 3rd ed.; Academic Press: San Diego, 2001; p 717.
(2) Atwood, J. L.; Davies, J. E. D.; MacNicol, D. D. *Inclusion Compounds*; Academic Press: New York, 1984; Vols. 1−3.
(3) Atwood, J. L.; Davies, J. E. D.; MacNicol, D. D. *Inclusion Compounds*; Oxford University Press: New York, 1991; Vols. 4−5.
(4) Hollingsworth, M. D. Harris, K. D. M. *Comprehensive Supramolecular Chemistry*; Pergamon: Oxford, 1996; Vol. 6.
(5) Harris, K. D. M. *Supramol. Chem.* **2007**, *19*, 47.
(6) Lefort, R.; Etrillard, J.; Toudic, B.; Guillaume, F.; Breczewski, T.; Bourges, P. *Phys. Rev. Lett.* **1996**, *77*, 4027–4030.
(7) Gopal, R.; Robertson, B. E.; Rutherford, J. S. *Acta Crystallogr., Sect. C: Cryst. Struct. Commun.* **1989**, *45*, 257.
(8) Greenfield, M. S.; Ronemus, A. D.; Vold, R. L.; Vold, R. R.; Ellis, P. D.; Raidy, T. R. *J. Magn. Reson.* **1987**, *72*, 89.
(9) Harris, K. D. M. *J. Mol. Struct.* **1996**, *374*, 241.
(10) Penner, G. H.; Polson, J. M.; Stuart, C.; Ferguson, G.; Kaitner, B. *J. Phys. Chem.* **1992**, *96*, 5121.
(11) Sidhu, P. S.; Penner, G. H.; Jeffrey, K. R.; Zhao, B.; Wang, Z. L.; Goh, I. *J. Phys. Chem. B* **1997**, *101*, 9087.
(12) Pan, Z.; Desmedt, A.; MacLean, E. J.; Guillaume, F.; Harris, K. D. M. *J. Phys. Chem. C* **2008**, *112*, 839.
(13) Prout, K.; Heyes, S. J.; Dobson, C. M.; McDaid, A.; Maris, T.; Muller, M.; Szaman, M. J. *Chem. Mater.* **2000**, *12*, 3561.
(14) Grottel, M.; Pajzderska, A.; Wąsicki, J. *Z. Naturforsch.* **2003**, *58a*, 638.
(15) Grottel, M.; Kozak, A.; Pajzderska, A.; Szczepański, W.; Wąsicki, J. *Z. Naturforsch.* **2004**, *59a*, 505.
(16) Małuszyńska, H.; Czarnecki, P. Z. *Kristallogr.* **2006**, *221*, 218.

(17) Palmer, B. A.; Kariuki, B. M.; Muppidi, V. K.; Hughes, C. E.; Harris, K. D. M. *Chem. Commun.* **2011**, *47*, 3760.
(18) Ilott, A. J.; Palucha, S.; Batsanov, A. S.; Harris, K. D. M.; Hodgkinson, P.; Wilson, M. R. *J. Phys. Chem. B* **2011**, *115*, 2791.
(19) Desmedt, A.; Kitchin, S. J.; Guillaume, F.; Couzi, M.; Harris, K. D. M.; Bocanegra, E. H. *Phys. Rev. B: Condens. Matter Mater. Phys.* **2001**, *64*, 054106.
(20) Toudic, B.; Rabiller, P.; Bourgeois, L.; Huard, M.; Ecolivet, C.; McIntyre, G. J.; Bourges, P.; Breczewski, T.; Janssen, T. *EPL* **2011**, *93*, 16003.
(21) Le Lann, H.; Odin, C.; Toudic, B.; Ameline, J. C.; Gallier, J.; Guillaume, F.; Breczewski, T. *Phys. Rev. B* **2000**, *62*, 5442.
(22) Jones, M. J.; Guillaume, F.; Harris, K. D. M.; Aliev, A. E.; Girard, P.; Dianoux, A.-J. *Mol. Phys.* **1998**, *93*, 545.
(23) Mueller, K. *J. Phys. Chem.* **1992**, *96*, 5733.
(24) Girard, P.; Aliev, A. E.; Guillaume, F.; Harris, K. D. M.; Hollingsworth, M. D.; Dianoux, A. J.; Jonsen, P. *J. Chem. Phys.* **1998**, *109*, 4078.
(25) Souaille, M.; Smith, J. C.; Guillaume, F. *J. Phys. Chem. B* **1997**, *101*, 6753.
(26) Vold, R. L.; Hoatson, G. L.; Subramanian, R. *J. Chem. Phys.* **1998**, *108*, 7305.
(27) Souaille, M.; Guillaume, F.; Smith, J. C. *J. Chem. Phys.* **1999**, *105*, 1529.
(28) Souaille, M.; Guillaume, F.; Smith, F. C. *J. Chem. Phys.* **1996**, *105*, 1516.
(29) Soetens, J.Ch.; Desmedt, A.; Guillaume, F.; Harris, K. D. M. *Chem. Phys.* **2000**, *261*, 125.
(30) Soetens, J.Ch.; Rice, W. R.; Brunaud, G.; Desmedt, A.; Guillaume, F. *Chem. Phys.* **2003**, *292*, 201.
(31) Małuszynska, H.; Czarnecki, P; Fojud, Z.; Wąsicki, J. *Acta Cystallogr., Sect. B* **2008**, *64*, 567.
(32) Pajzderska, A.; Gonzalez, M. A.; Wąsicki, J. *J. Chem. Phys.* **2008**, *128*, 084507.
(33) Pajzderska, A.; Fojud, Z.; Goc, R.; Wasicki, J. *J. Phys.: Condens. Matter* **2007**, *19*, 156220.
(34) Pajzderska, A.; Czarnecki, P.; Embs, J. P.; Gonzalez, M. A.; Juranyi, F.; Krawczyk, J.; Peplińska, B.; Wąsicki, J. *Phys. Chem. Chem. Phys.* **2011**, *13*, 8908.
(35) Mukhopadhyay, R.; Mitra, S.; Tsukushi, I.; Ikeda, S. *Chem. Phys. Lett.* **2001**, *341*, 45.
(36) http://www.ill.eu/instruments-support/computing-for-science/cs-software/all-software/lamp/
(37) Bee M. *Quasielastic Neutron Scattering: Principles and Applications in Solid State Chemistry, Biology, and Material Science*; Adam Hilger: Bristol and Philidelphia, 1988.
(38) Bée, M. *Phys. B (Amsterdam, Neth.)* **1992**, *182*, 323.
(39) Yildirim, T.; Gehring, P. M.; Neumann, D. A.; Eaton, P. E.; Emrick, T. *Phys. Rev. B* **1999**, *60*, 314.
(40) Hempelmann R. *Quasielastic Neutron Scattering and Solid State Diffusion*; Oxford Series on Neutron Scattering in Condensed Matter, 13; Oxford University Press: New York, 2000.
(41) Toudic, B.; Lechner, R. E. *J. Phys. C: Solid State Phys.* **1984**, *17*, 5503.
(42) *International Tables for Crystallography. Vol. D, Physical Properties of Crystals*; Authier, A., Ed.; Kluwer Academic Publishers: Dordrecht and Boston, 2003.
(43) Prout, K. *Croat. Chem. Acta* **2002**, *75*, 817.
(44) Lechner, R. E. *Phys. B (Amsterdam, Neth.)* **2001**, *301*, 83.
(45) Ripmeester, J. A. *Can. J. Chem.* **1976**, *54*, 3453.
(46) Lewicki, S.; Wąsicki, J.; Czarnecki, P.; Szafraniak, I.; Kozak, A.; Pająk, Z. *Mol. Phys.* **1998**, *94*, 973.